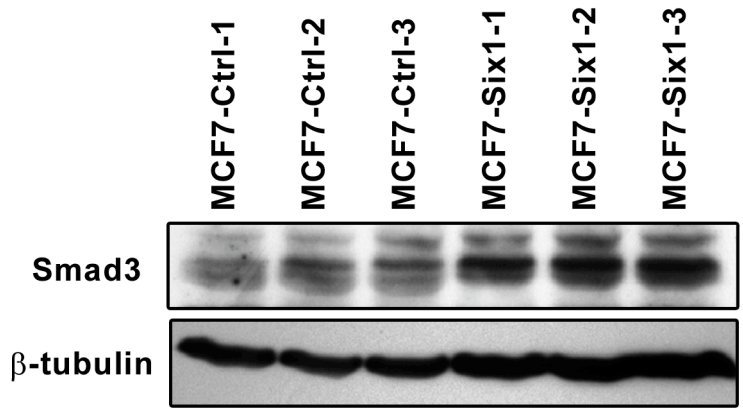

Supplementary Figure 1 Western blot analysis of total Smad3 levels from whole cell lysates of MCF7-Ctrl and MCF7-Six1 cells

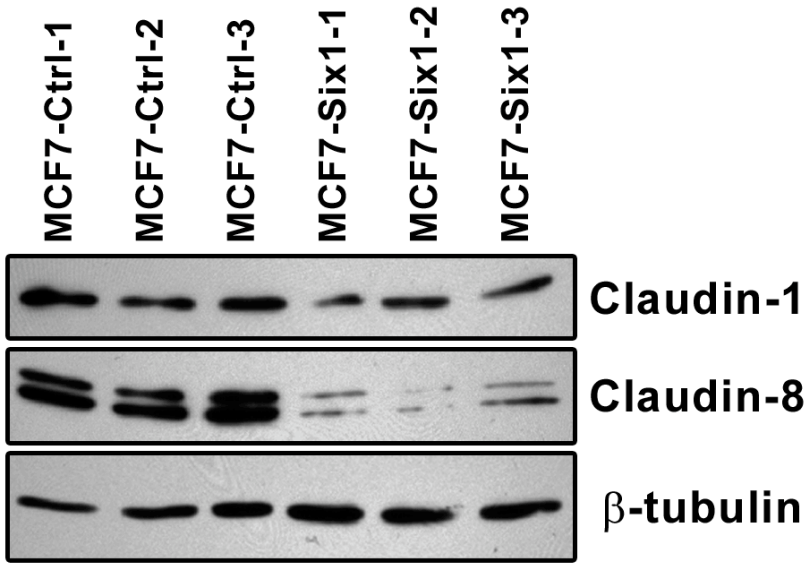

Supplementary Figure 2 MCF7-Six1 clones display decreased claudin-1 and claudin-8 as determined by western blot of whole cell lysates

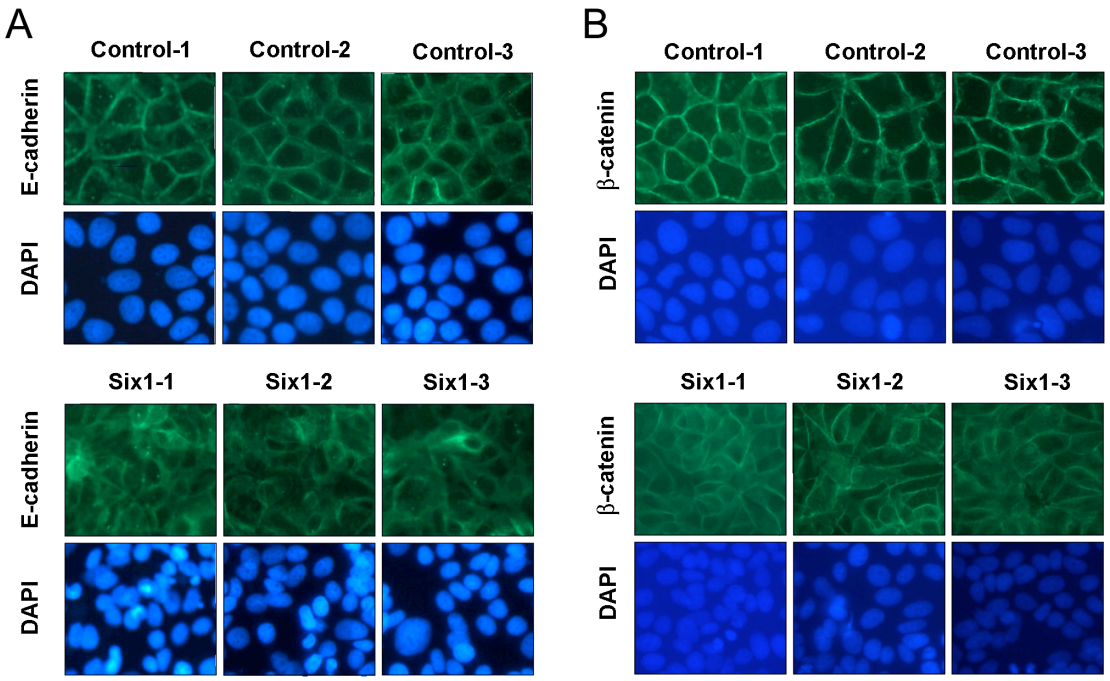

Supplementary Figure 3 Six1 induces a relocalization of the E-cadherin and β-catenin. (A) Immunofluorescent staining of MCF7-Six1 and Ctrl clones for E-cadherin (above) and DAPI staining (below). (B) Immunofluorescent staining of MCF7-Six1 and Ctrl clones for β-catenin (above) and DAPI staining (below).

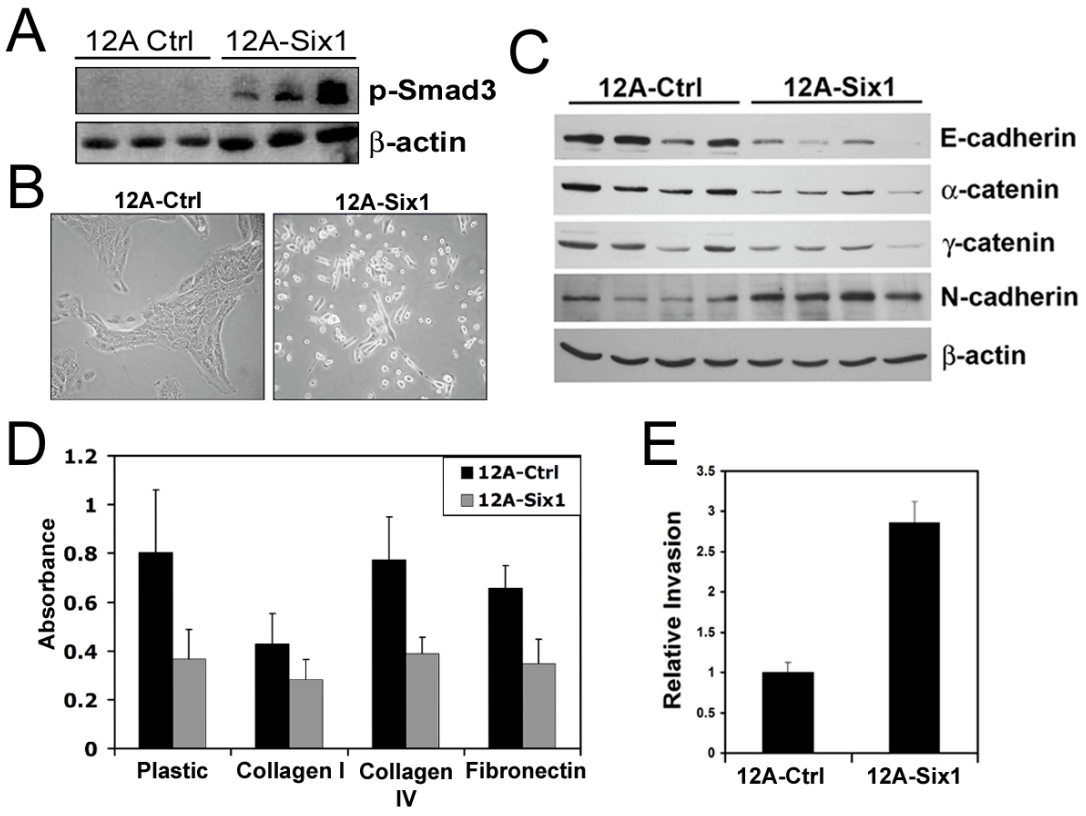

Supplementary Figure 4 Six1 induces increased TGF-β signaling and EMT in immortalized, but nontransformed mammary epithelial cells. (A) Western blot of 12A-Ctrl or 12A-Six1 cells shows increased levels of phosphorylated Smad3 in Six1 expressing cells. (B) Stable Six1 expression in MCF12A cells induces a loss of epithelial morphology as determined by phase contrast microscopy. (C) Western blot from 12A-Ctrl or 12A-Six1 clones shows reduced expression of the epithelial markers E-cadherin, α-catenin, and γ-catenin, and increased expression of the mesenchymal marker N-cadherin. (D) 12A-Six1 clones show decreased cell-matrix adhesion, with the relative number of adhering cells quantified by crystal violet staining. (E) Six1 expression increases *in vitro* invasion. For panels (D, E) data are represented as mean +/- SD of 3 individual clones.

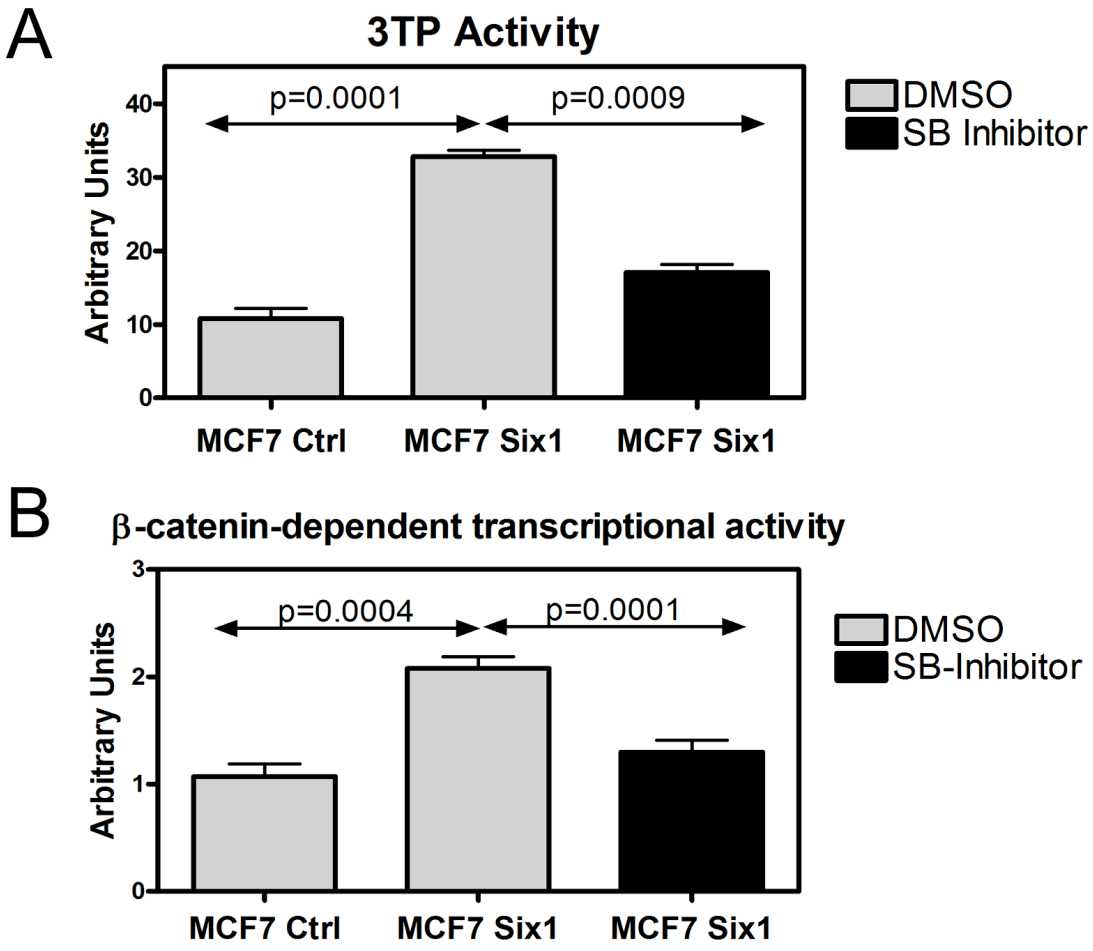

Supplementary Figure 5 Pharmacologic inhibition of TGF-β signaling reverses elements of Six1-induced EMT (A) Treatment of the MCF7-Six1 clones with 3uM SB-431542 TβRI kinase inhibitor for 24 hours decreases TGF-β signaling to levels comparable to the MCF7-Ctrl clones as assessed by the TGF-β responsive 3TP-reporter and normalized to Renilla luciferase (B) Treatment of the MCF7-Six1 clones with 3uM SB-431542 TβRI kinase inhibitor for 24 hours reverses β-catenin dependent transcription as assessed by the β-catenin-responsive TOP-FLASH reporter and normalized to Renilla luciferase. Data are represented as mean +/- SD of three individual clones.

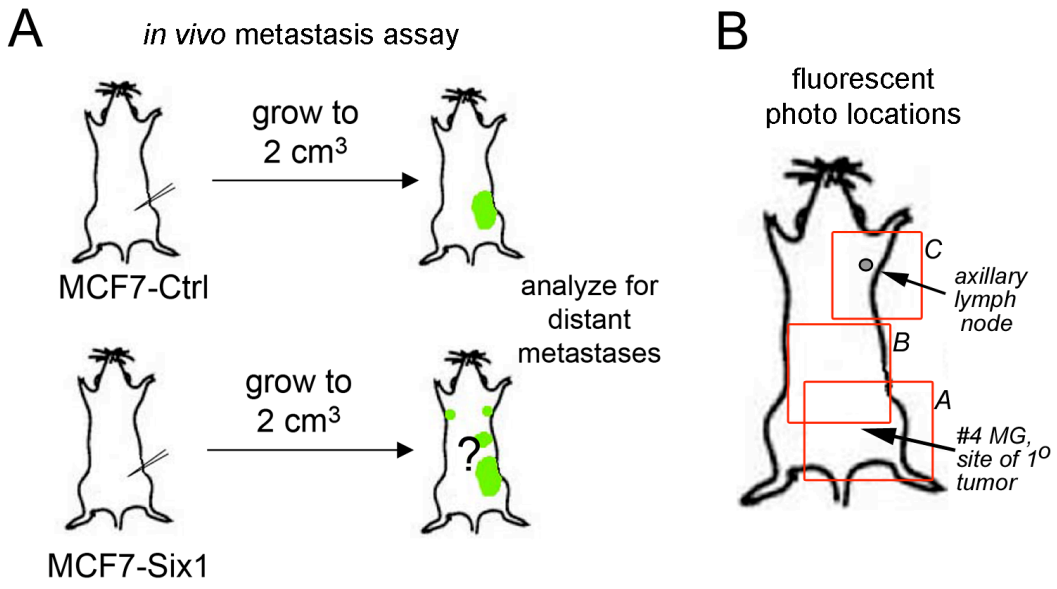

Supplementary Figure 6 (A) Diagrammatic representation of the Six1 metastasis model. Control and Six1-expressing stable clones were injected orthotopically into nude and NOD/Scid mice and primary tumors were allowed to grow to a uniform size before analysis for metastatic spread of fluorescently labeled tumor cells. (B) Diagram indicates the location of fluorescence photography images shown in figure 6 A-C.

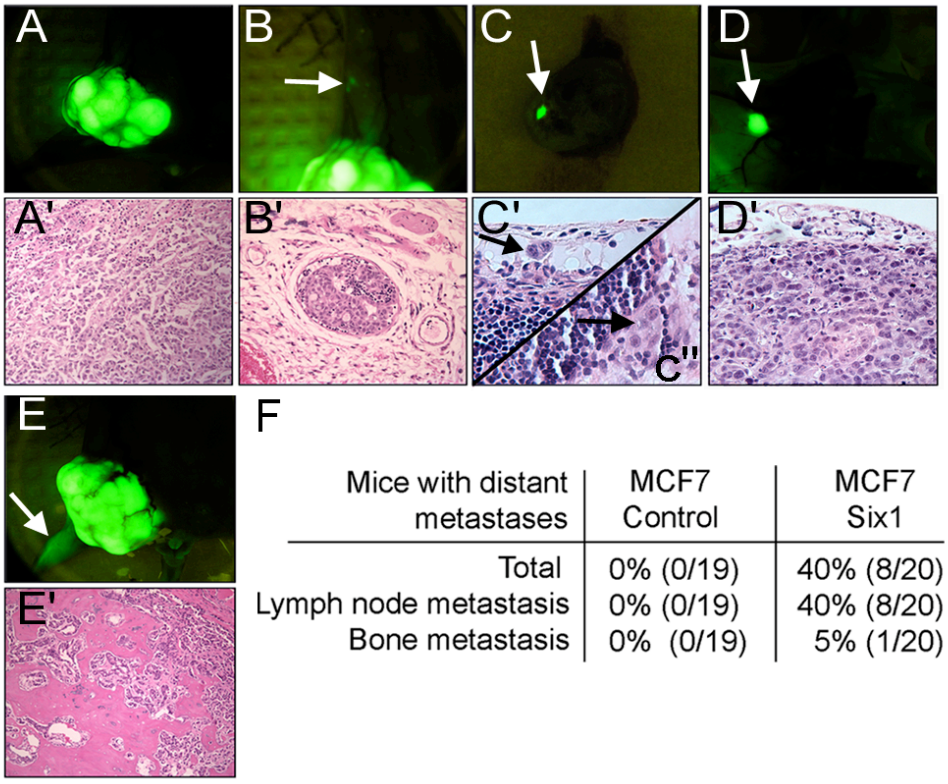

Mice with distant metastases	MCF7 Control	MCF7 Six1
Total	0% (0/19)	40% (8/20)
Lymph node metastasis	0% (0/19)	40% (8/20)
Bone metastasis	0% (0/19)	5% (1/20)

Supplementary Figure 7 Six1 overexpression induces metastasis in an orthotopic xenograft model. (A-E) Nude mice with MCF7-Six1 tumors, but none of the control mice, exhibited distant metastases to lymph nodes and bone, as detected by whole body imaging of ZsGreen fluorescence (upper panels) and confirmed in a subset of tumors by histology (H&E stain; lower panels). (A) Representative primary tumor, showing a poorly differentiated carcinoma (A'). (B and B') Tumor cells within lymphatic vessels away from primary tumor. (C, C' and C'') Tumor deposits within distant lymph nodes (black arrows: tumor cells in subcapsular sinus [C'] and subcapsular lymphoid tissue [C'']). (D and D') Large axillary metastasis, consistent with lymph node replaced by tumor. (E and E') Bone metastasis in the femur of one mouse. (F) Summary of Six1 xenograft tumor metastasis data.